CHAPTER V

RESULTS AND DISCUSSION

X-Ray Diffraction Patterns(XRD)

The X-ray diffraction patterns of all the catalysts prepared are shown in Figure 5.1-5.6. The XRD patterns of SAPO-5, SAPO-11 and SAPO-34 from patent literature are also demonstrated for comparison. XRD patterns of the catalysts were determined on an X-ray diffractometer with Ni-filtered CuKα radiation at an angle 2θ ranging from 70 to 7 degree. The comparisons of the individual patterns with those from the patent literature due to the effect of the amounts of TEAOH, SiO_2, H_3PO_4, and HF as well as the time of crystallization were described below.

1. Effect of TEAOH Amount on SAPO-34 Synthesis

The XRD patterns of the catalysts prepared by using different amounts of TEAOH are shown in Figure 5.1. When 0.5 mole of TEAOH was used some characteristic peaks of SAPO-5 were found. At 1.0 mole of TEAOH, the pure phase of SAPO-34 was obtained; however, its crystallinity was considerably low. When the amount of TEAOH was raised to 1.3 moles, the monophasic SAPO-34 with higher crystallinity was achieved. However, when the amount of TEAOH was increased to 1.5 mole, the resulting mixture became suspension and only few amount of crystallized solid was obtained.

A templating theory has been postulated for the role of the cation in stabilizing the formation of structural subunits thought to be precursors of

crystalline species in the reaction mixture. Although the exact mechanism of the templating effect still is not fully understood, it is visualized that the structure grows around the template, thus stabilizing certain pore structure or subunits. When too excess amount of TEAOH was used, the crystallization poorly occured. It is suspected that the nuclei scattered around the template and suspended in the mixture, thus few amounts of crystallite solid. It should be noted that a kind of template may facilitate the crystallization of catalysts more than one structure. In addition to the amount of template, the composition range of other ingredients as well as the crystallization temperature were believed to control the crystallization of a certain structure of catalyst.

2. Effect of Si Amount on SAPO-34 synthesis

The XRD patterns of the catalysts prepared by using different amount of cataloid (30% SiO_2) are shown in Figure 5.2. At 0.6 mole of cataloid, SAPO-34 only was obtained. When the amounts of cataloid were raised to 1.0, 1.5, and 2.0 moles, some characteristic peaks of SAPO-11 were observed.

The excess amount of silicon may increase the formation of Si-O-Si subunits in the framework resulting in obtaining SAPO-11 instead of SAPO-34.

3. Effect of Phosphorous Amount on SAPO-34 Synthesis

As shown in Figure 5.3, The XRD patterns of the catalyst prepared by using 1.5 mole H_3PO_4 showed the pure crystalline SAPO-34 though its crystallinity was considerbly low. At 2.0 moles of H_3PO_4 used the crystallinity increased; however, further enhancement of H_3PO_4 amounts to 2.5 and 3.0 caused the formation of co-crystallized SAPO-5.

The excess amount of phosphorous may increase the formation of Al-O-P subunits in the catalyst framework and thus SAPO-5 was obtained predominantly.

4. Effect of HF Addition on the Enhancement of Crystallinity

From the results shown in Figure 5.1-5.3, it has been concluded that when the amount of Al was fixed at 2 moles ; 1.3 moles of TEAOH, 0.6 mole of cataloid, and 2 moles of H_3PO_4 were required for the monophasic formation of SAPO-34. Less success has been found in increasing the crystallinity of SAPO-34 by varying the catalyst compositions. Thus further attempt has been made by adding HF in different amounts to the catalyst during gel formation. As shown in Figure 5.4, the crystallinity of monophasic SAPO-34 increased with the increasing amount of HF. The optimum amount of HF added to increase the crystallinity was 0.5 mole, higher than which caused the formation of some SAPO-5 as seen from the small peak around 8°.

Since it has been well known that the fluoride ion acts as the templating agent for the crystallization of ZSM-5 [94]. The presence of F^{-1} ion may play an important role as the co-template with TEAOH for the crystallization of SAPO-34. It is believed that F^{-1} ion may increase the rate of crystallization and, subsequently, the small crystallite size was obtained with high crystallinity.

5. Effect of Crystallization Time on SAPO-34 Synthesis

The XRD patterns of the catalysts crystallized at 200 °C for 4 h, 24 h, and 72 h, respectively are shown in Figure 5.5. It has been shown that prolonged crystallization over 4 h has no significant effect on crystallinity increase. Thus 4 h of crystallization at 200 °C was enough for SAPO-34 synthesis with high crystallinity.

The time required for the crystallization of SAPO-34 should depend on the crystallization temperature and the nature of the structure directing agent used. TEAOH and HF may facilitate the crystallization of SAPO-34 well enough at 200 °C within 4 h and thus further prolonged operation has no significant effect.

6. Comparison of XRD patterns of the prepared catalyst with those of patent literature

The XRD patterns of the optimum formula of SAPO-34, i.e., 2 moles of Al ; 1.3 moles of TEAOH; 0.6 mole of cataloid; and 2 moles of H_3PO_4 prepared in the laboratory by rapid crystallization method, was almost the same as that of patent literature [93]. This indicates the sucessful synthesis of SAPO-34 with the framework topology of the natural zeolite chabazite.

The addition of HF did not change the XRD patterns of the catalysts but increase their crystallinity. This means the high crystallinity of SAPO-34 can be obtained by using TEAOH and HF as the structure directing agents.

Specific Surface Area

The BET surface area of the catalysts was calculated on the basis of N_2 adsorption measured by the flow method using a gas chromatograph at the liquid N_2 temperature. As show in Table 5.1, the BET surface areas of all SAPO-34/HF were in the same range as that of SAPO-34 catalyst. This is consistent with the above-mentioned result that the XRD patterns of all the prepared catalysts are almost the same as that of SAPO-34 catalyst. This indicates that HF does not affect the change in BET surface area of the catalysts. Table 5.1 shows BET surface areas of SAPO-34, SAPO-34/0.2 mole

Figure. 5.1 XRD patterns of catalysts containing different amounts of TEAOH

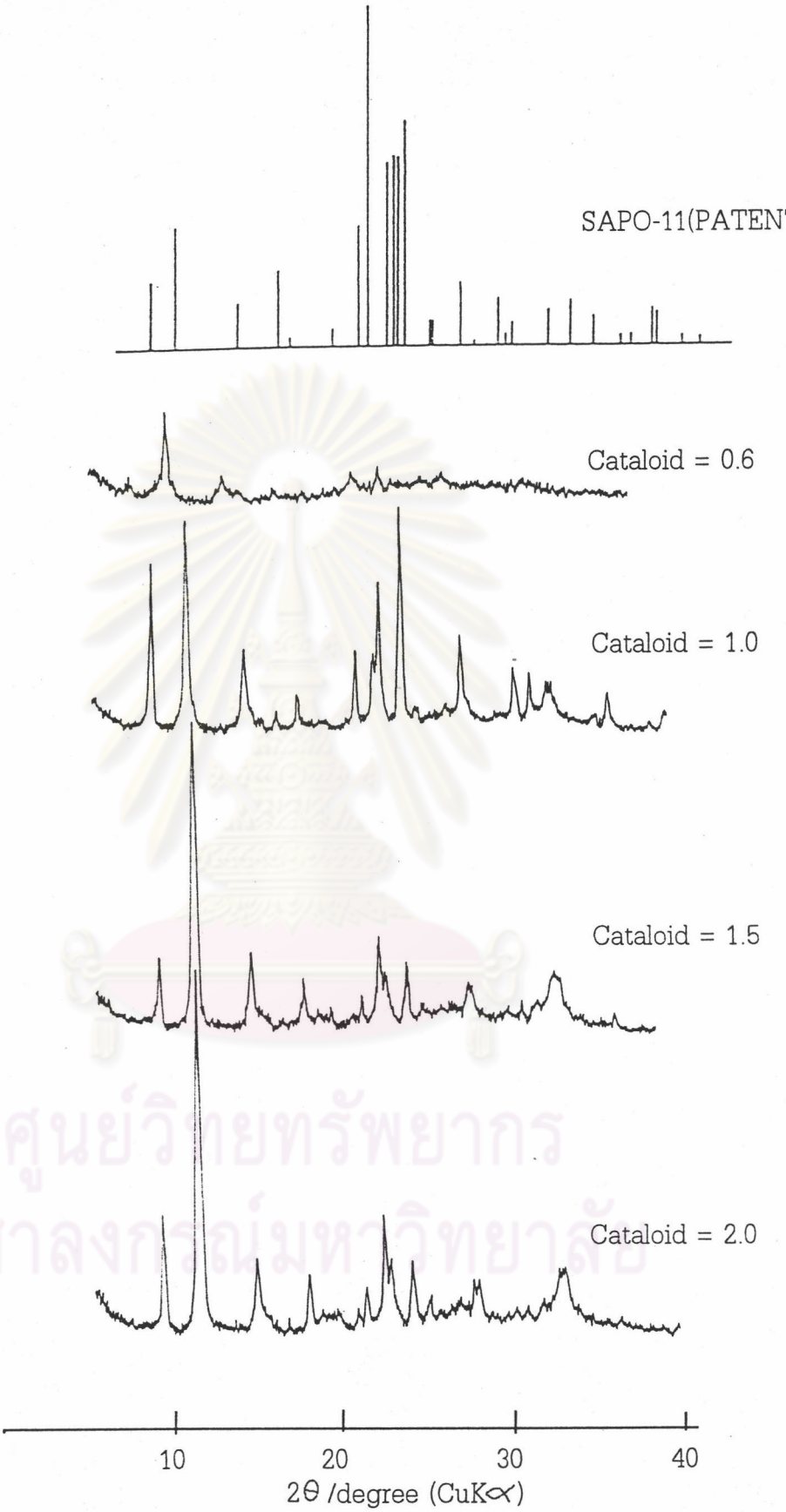

Figure. 5.2 XRD patterns of catalysts containing different amounts of cataloid.

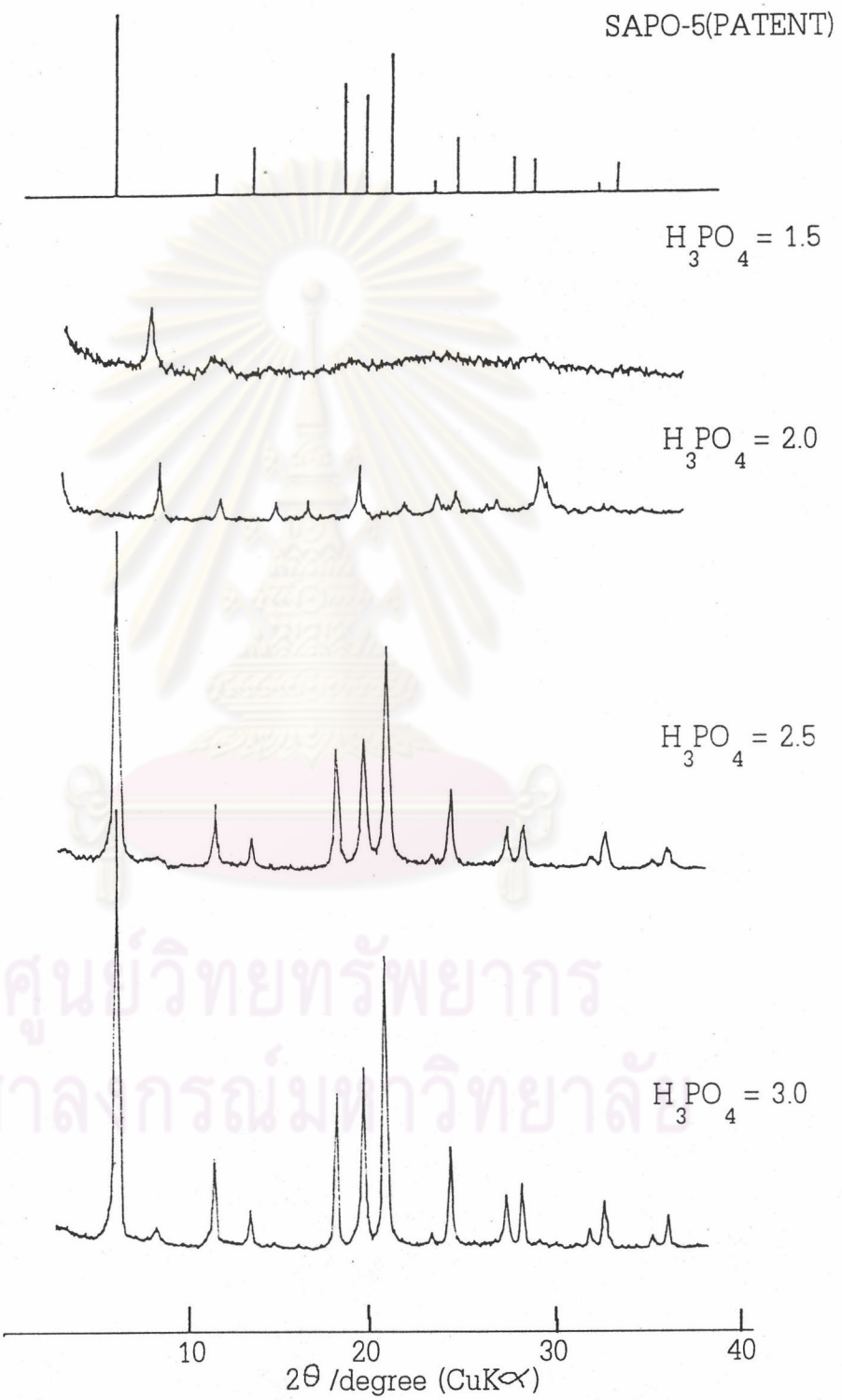

Figure. 5.3 XRD patterns of catalysts containing different amounts of H_3PO_4

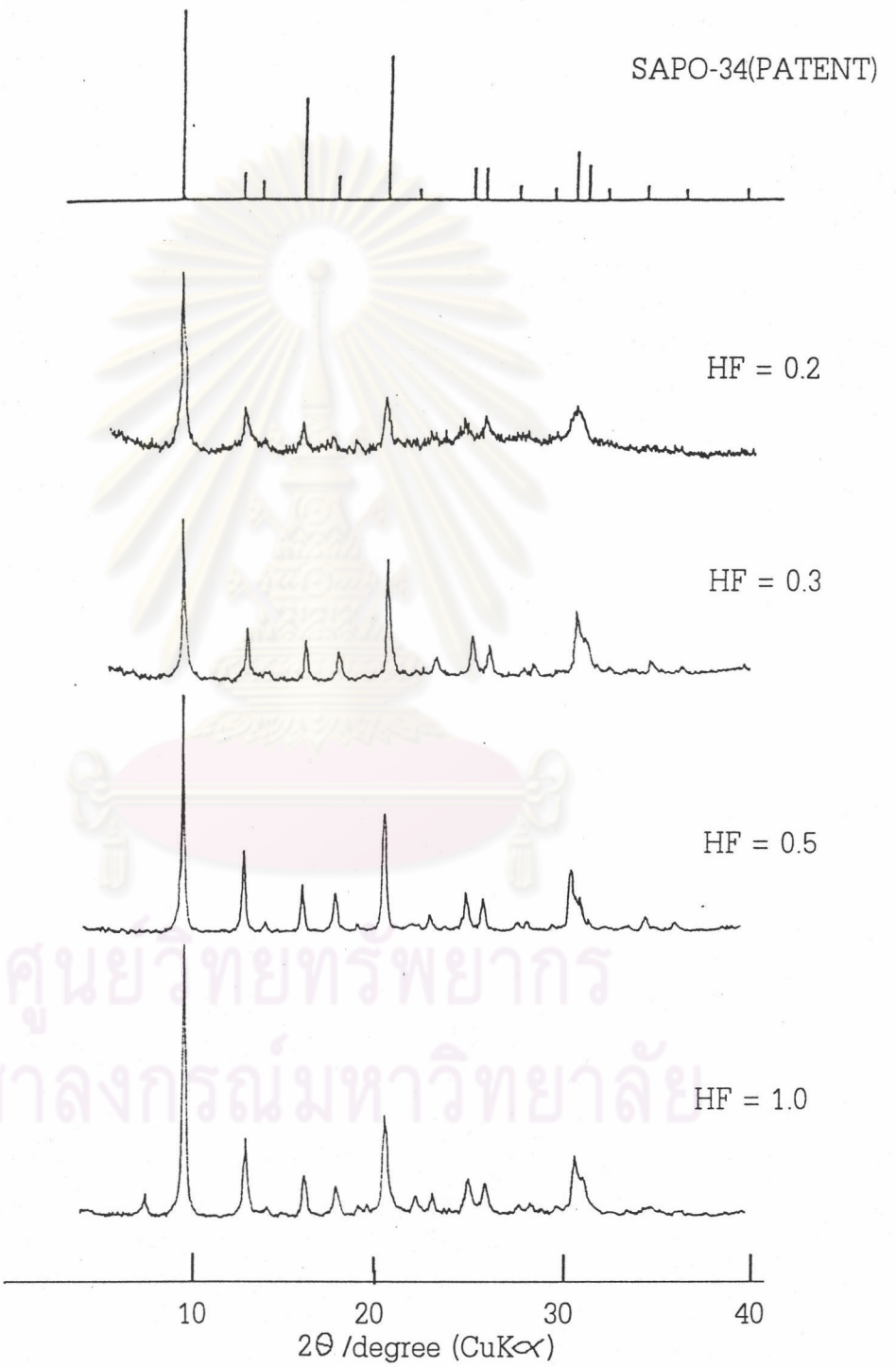

Figure. 5.4 XRD patterns of catalysts containing different amounts of HF

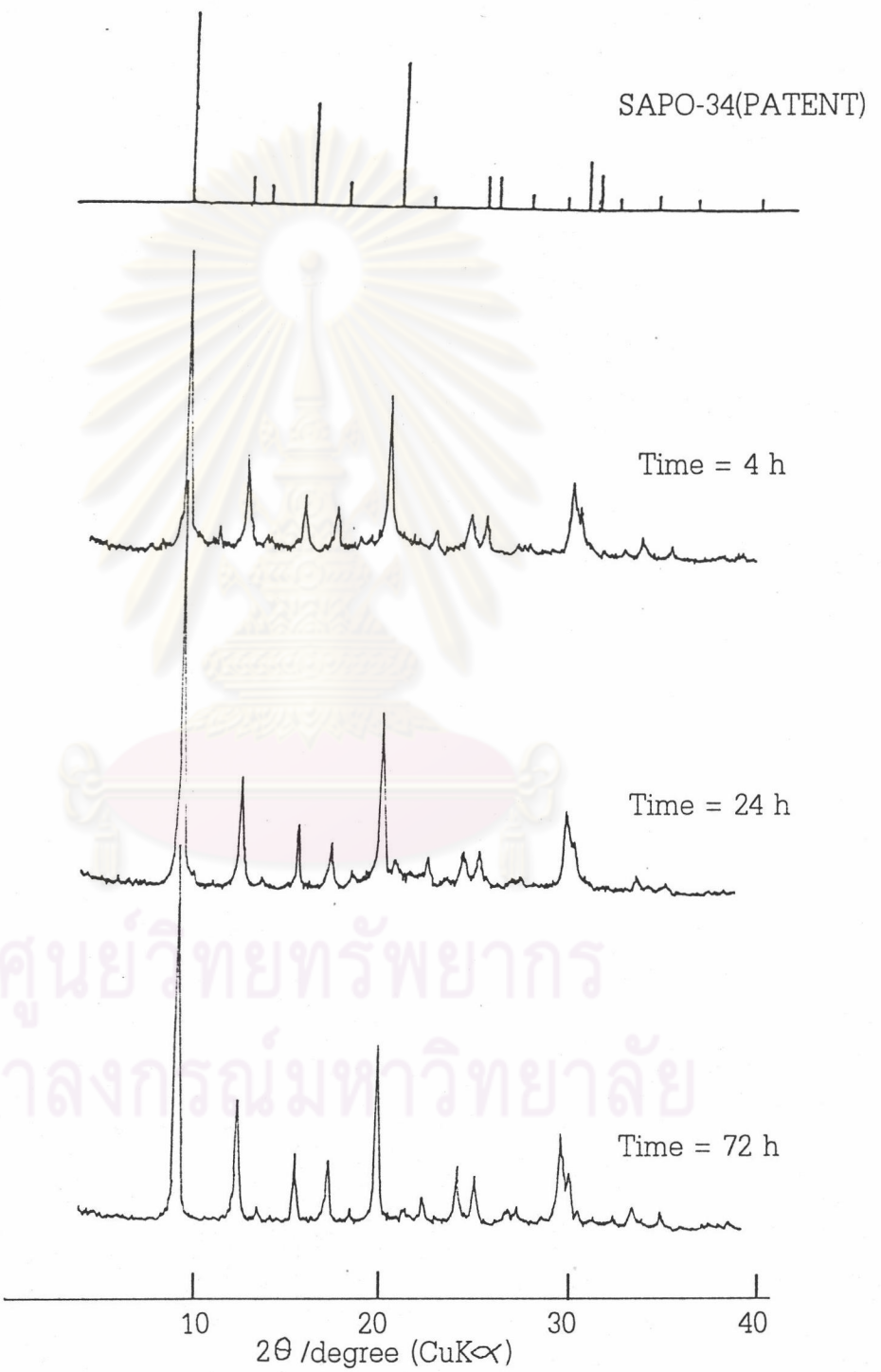

Figure. 5.5 XRD patterns of SAPO-34 crystallized at 200 °C for different hours.

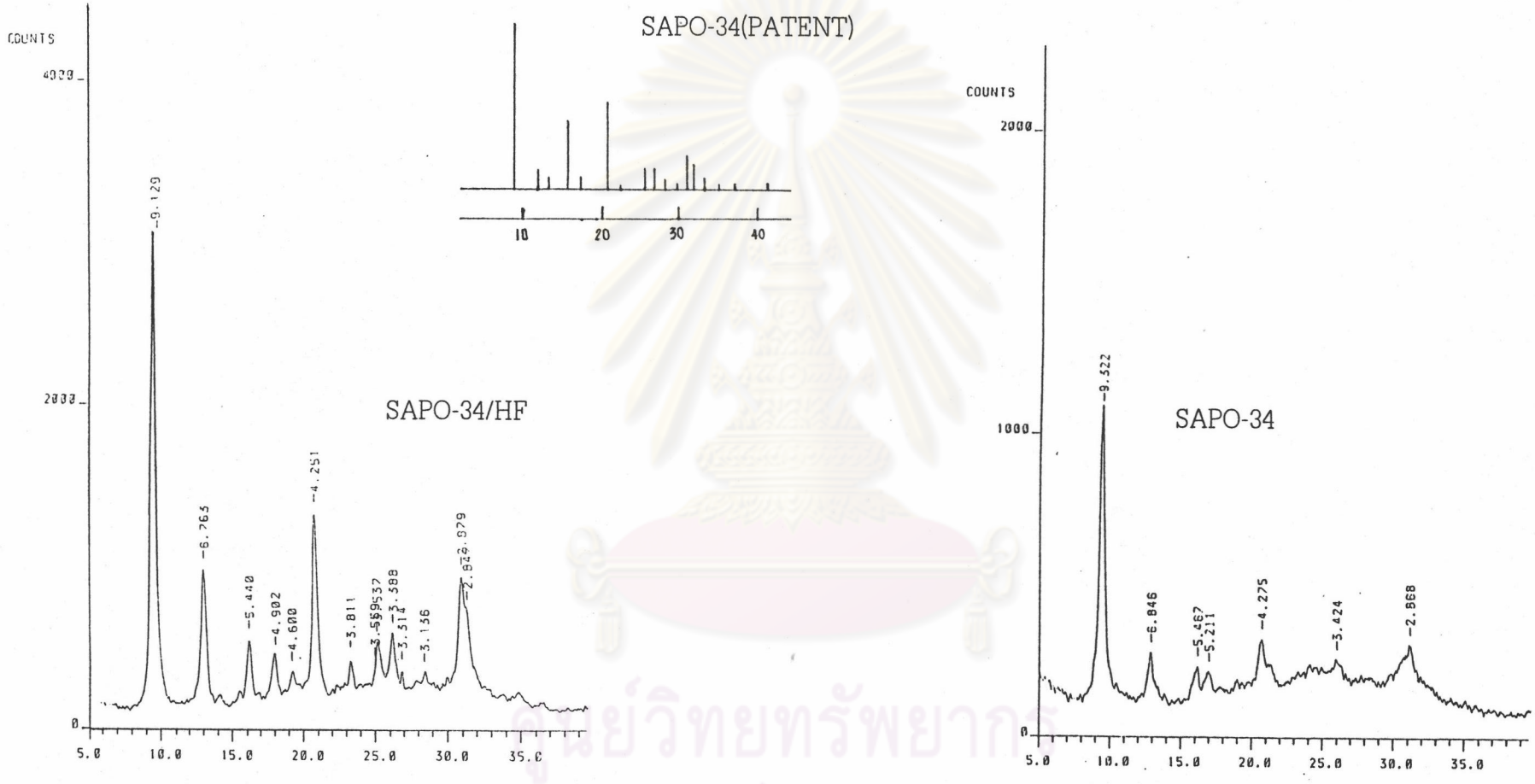

Figure 5.6 XRD patterns of SAPO-34/HF and SAPO-34 compared with patent literature.

HF, SAPO-34/0.3 mole HF, SAPO-34/0.5 mole HF and SAPO-34/1.0 mole HF.

Table 5.1 BET surface area of the catalysts

Catalysts	BET surface areas (m^2 /g of catalyst)
SAPO-34	570
SAPO-34/0.2 mole HF	568
SAPO-34/0.3 mole HF	589
SAPO-34/0.5 mole HF	574
SAPO-34/1.0 mole HF	575

Morphology

Morphologies of the crystals were observed with a JEOL scanning electron microscope (SEM). SEM photographs of the catalysts are shown in Figure 5.7. All the catalysts were composed of cubic crystals of uniform size. This crystal habit is typical for the chabazite structure.

Acidity

The acidity of catalysts was assessed by temperature-programmed desoption (TPD) of NH_3 determined on a Rigaku Thermal Analyzer TG 8110 equipped with Thermal Analysis Station TAS 100. The profiles for TPD of NH_3 form SAPO-34 and SAPO-34/HF are shown in Figure 5.8. These profiles have two peaks, one at a low temperature rang around 130-150 $^{\circ}$C and the other at a

(a)

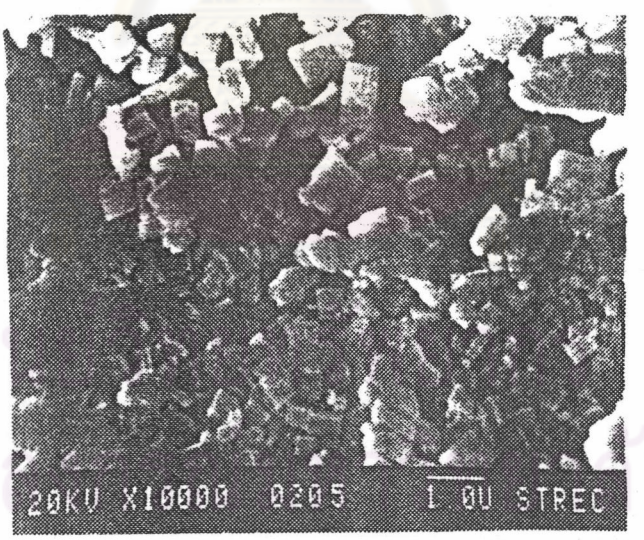

(b)

Figure 5.7 SEM photographs of SAPO-34 (a) and SAPO-34/HF (b)

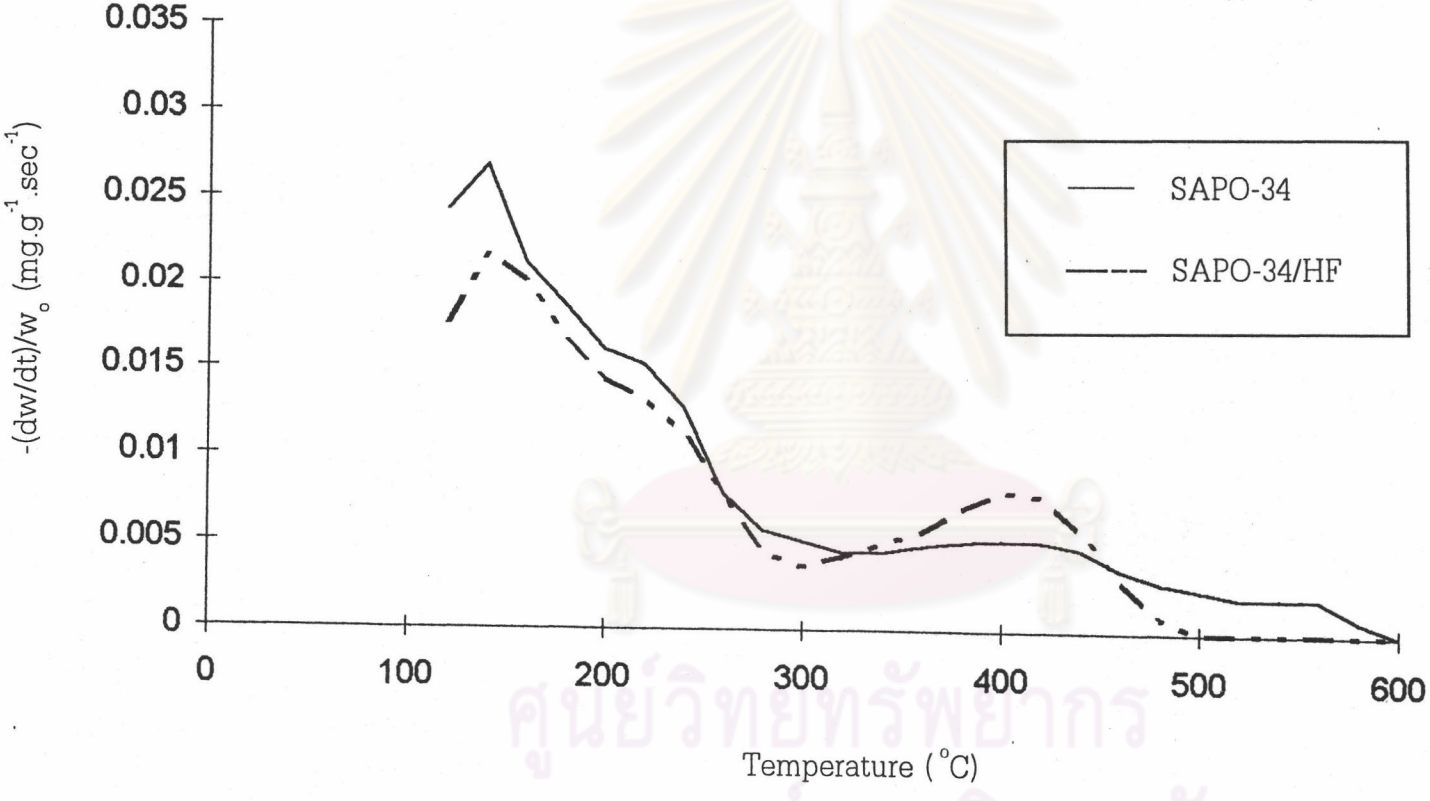

Figure 5.8 TPD profile of desorbed NH_3 from SAPO-34 and SAPO-34/HF.

high temperature range around 380-420 °C, and are similar to the NH_3-TPD profiles for the microporous crystals having strong acid sites such as a typical H-ZSM-5. The low and high temperature peaks correspond to weak and strong acid sites, respectively. the high temperature peak of SAPO-34/HF was greater than that of SAPO-34 catalyst.

Methanol conversion to Light Olefins Reaction

1. Effect of TEAOH Amounts on Hydrocarbon Distribution

The methanol conversion to light olefins was carried out at GHSV 2,000 h^{-1}, temperature 450 °C, feed gas mixture of 20% MeOH balanced with 80% N_2 and 1 h time on stream. Hydrocarbon distribution on the catalysts containing different amounts of TEAOH is shown in Figure 5.9. All the catalyst exhibited high selectivity to light olefins; however, selectivity to ethylene increased with the increasing amount of TEAOH. It has been clearly shown that with the presence of SAPO-5 in the catalyst structure, the production of propylene was dominant to that of ethylene. SAPO-34 having chabazite structure should be responsible for the high selectivity of ethylene.

2. Effect of HF Amounts on Hydrocarbon Distribution

Hydrocarbon distribution of methanol conversion, with the same condition as mentioned above, on the catalysts having different amounts of HF is shown in Figure 5.10. The selectivity for ethylene increased with the increasing amounts of HF. The ethylene selectivity as high as 58% was achieved on SAPO-34 containing 0.5 mole of HF. The high selectivity for ethylene should be attributed to the high crystallinity of pure phase of SAPO-34.

3. Effect of GHSV on Hydrocarbon Distribution

Figure 5.11 shows the hydrocarbon distribution of methanol conversion on SAPO-34 having the optimum compositions, namely, 2 moles of Al, 1.3 moles of TEAOH, 0.6 mole of cataloid, 2 moles of H_3PO_4, and 0.5 mole of HF with various GHSV ranging from 2,000-10,000 h^{-1}. No significant change in hydrocarbon distribution was observed during the increase of GHSV. However, at GHSV higher than 2,000 h^{-1} , little amounts of methanol remained unreacted and some amounts of dimethyl ether (DME) were found. Thus the methanol conversion reaction must proceed via dimethyl ether as an intermediate following the mechanism:

$$2CH_3OH \longleftrightarrow CH_3OCH_3 + H_2O \quad (5.1)$$

$$CH_3OCH_3 \longleftrightarrow CH_2=CH_2 + H_2O \quad (5.2)$$

$$CH_2=CH_2 + CH_3OH \longleftrightarrow CH_3-CH=CH_2 + H_2O \quad (5.3)$$

4. Effect of Reaction Temperatures on Hydrocarbon Distribution

Hydrocarbon distribution of methanol conversion on the optimum SAPO-34 at various reaction temperatures is shown in Figure. 5.12. The methanol conversion was carried out at GHSV 2,000 h^{-1}, by using feed gas mixture of 20% MeOH and 80% N_2 for 1 h time on stream. During the whole temperature range (250, 300, 350, 400, 450, 500, 550 and 600 °C) tested, at the the temperatures lower than 400 °C, some methanol remained unreacted and the formation of ethylene was less dominant than that of propylene. Some amounts of dimethyl ether were also observed during 250-300 °C. From 450 °C the complete conversion of methanol was achieved and ethylene selectivity was greater than propylene selectivity.

Since the formation of propylene was more thermodynamically favorable than that of ethylene, as seen from their Gibbs free energy, the ethylene selectivity increased with the increasing temperature.

$$CH_3OCH_3 \longleftrightarrow CH_2{=}CH_2 + H_2O \qquad \Delta G^O = -47.61$$

$$CH_2{=}CH_2 + CH_3OH \longleftrightarrow CH_3{-}CH{=}CH_2 + H_2O \quad \Delta G^O = -71.55$$

However, at the temperatures higher than 500 °C, the considerable amounts of methane were formed resulting in the decline in ethylene selectivity. Thus the optimum temperature of methanol conversion to obtain high ethylene selectivity was 450-500 °C.

5. Effect of Methanol Compositions on Hydrocarbon Distribution

Figure 5.13 shows the hydrocarbon distribution of methanol conversion on SAPO-34 by varying methanol compositions. The total conversion of methanol was maintained even at 30% methanol. However, the ethylene selectivity decreased slightly equlibrium of the at high methanol compositions. The increasing amount of methanol shifted the reaction below to the right and thus increased the formation of propylene:

$$CH_2{=}CH_2 + CH_3OH \longleftrightarrow CH_3{-}CH{=}CH_2 + H_2O$$

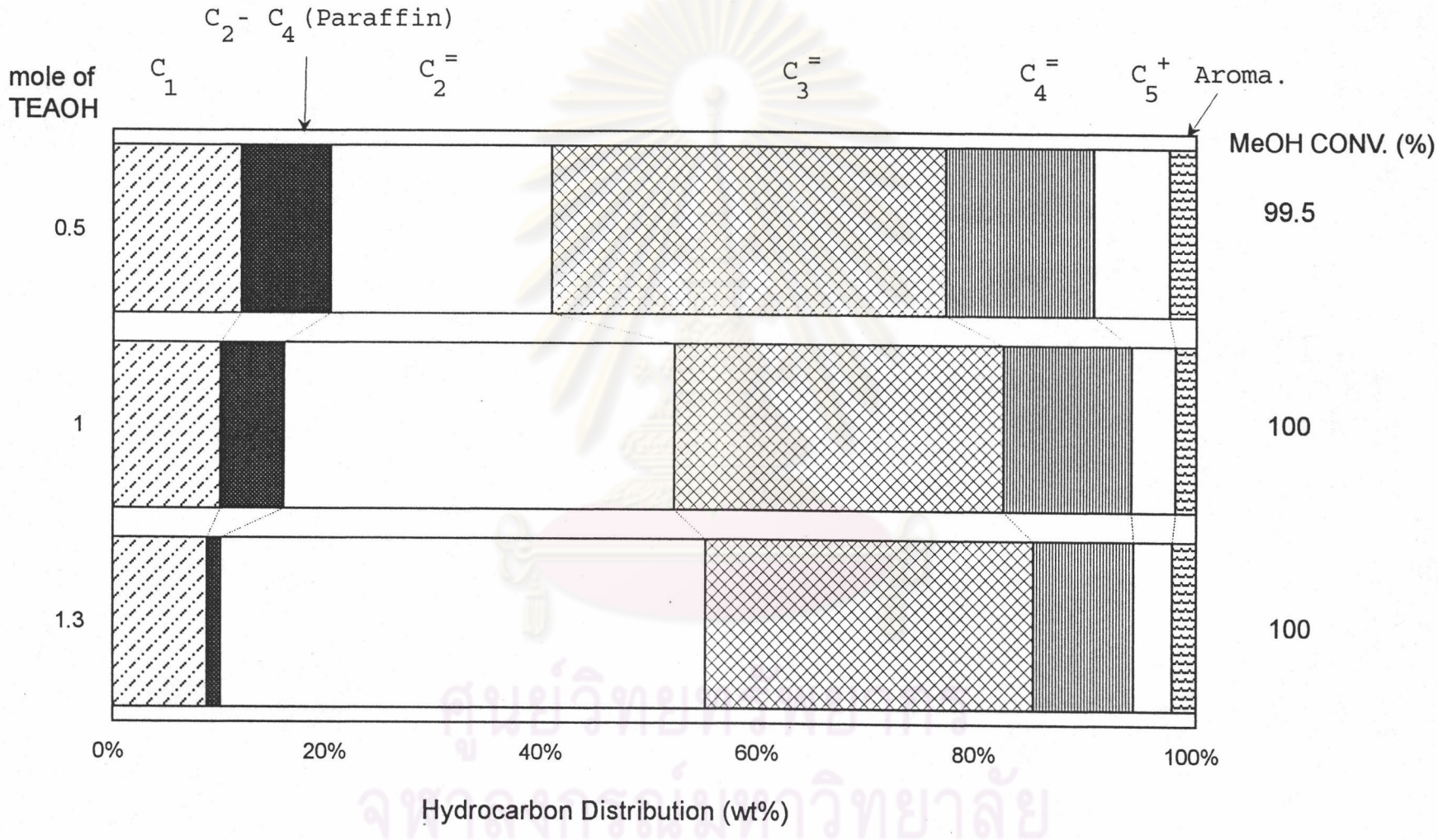

Figure 5.9 Hydrocarbon distribution of methanol conversion on catalysts having different amounts of TEAOH

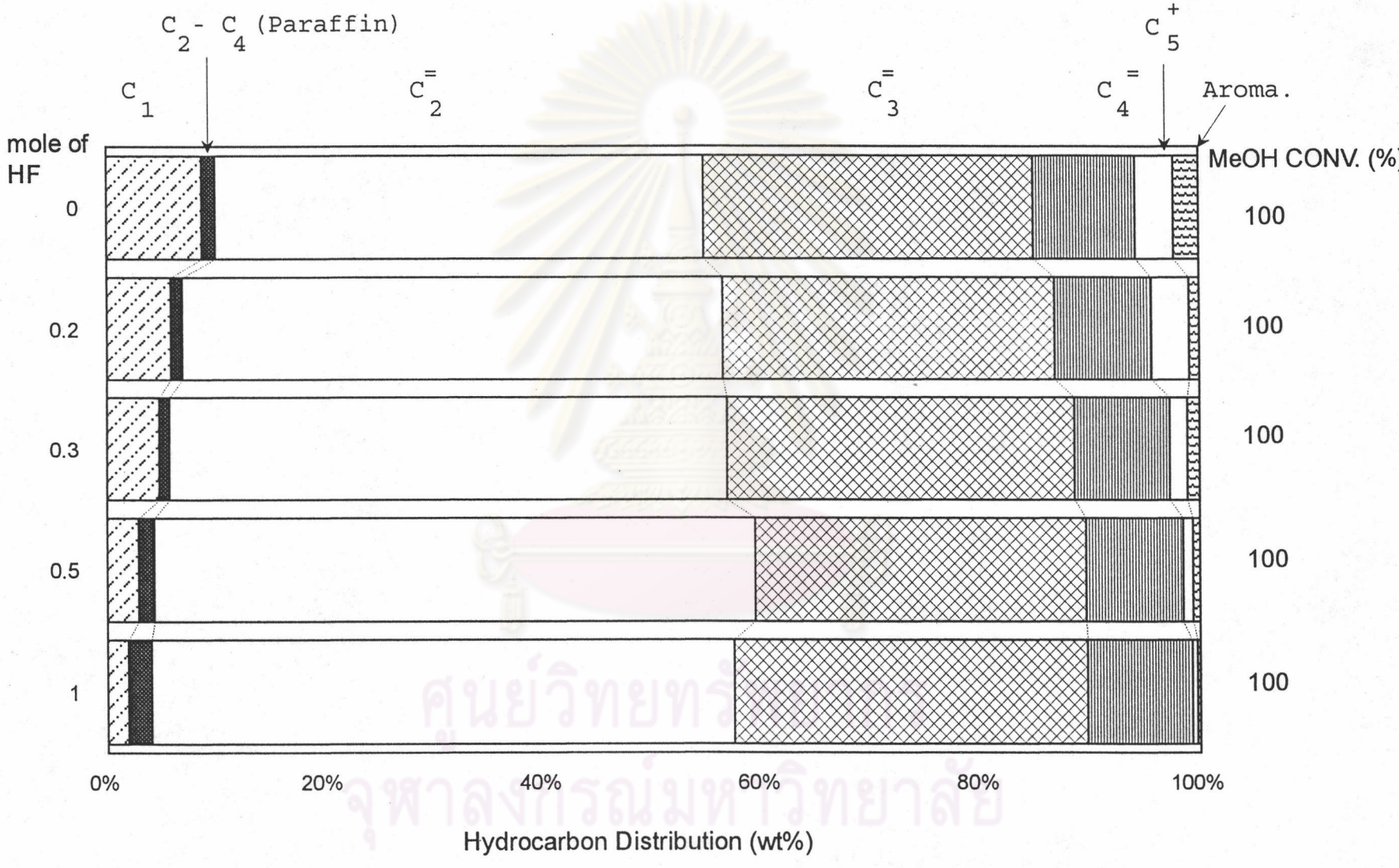

Figure 5.10 Hydrocarbon distribution of methanol conversion on SAPO-34 having different amounts of HF.

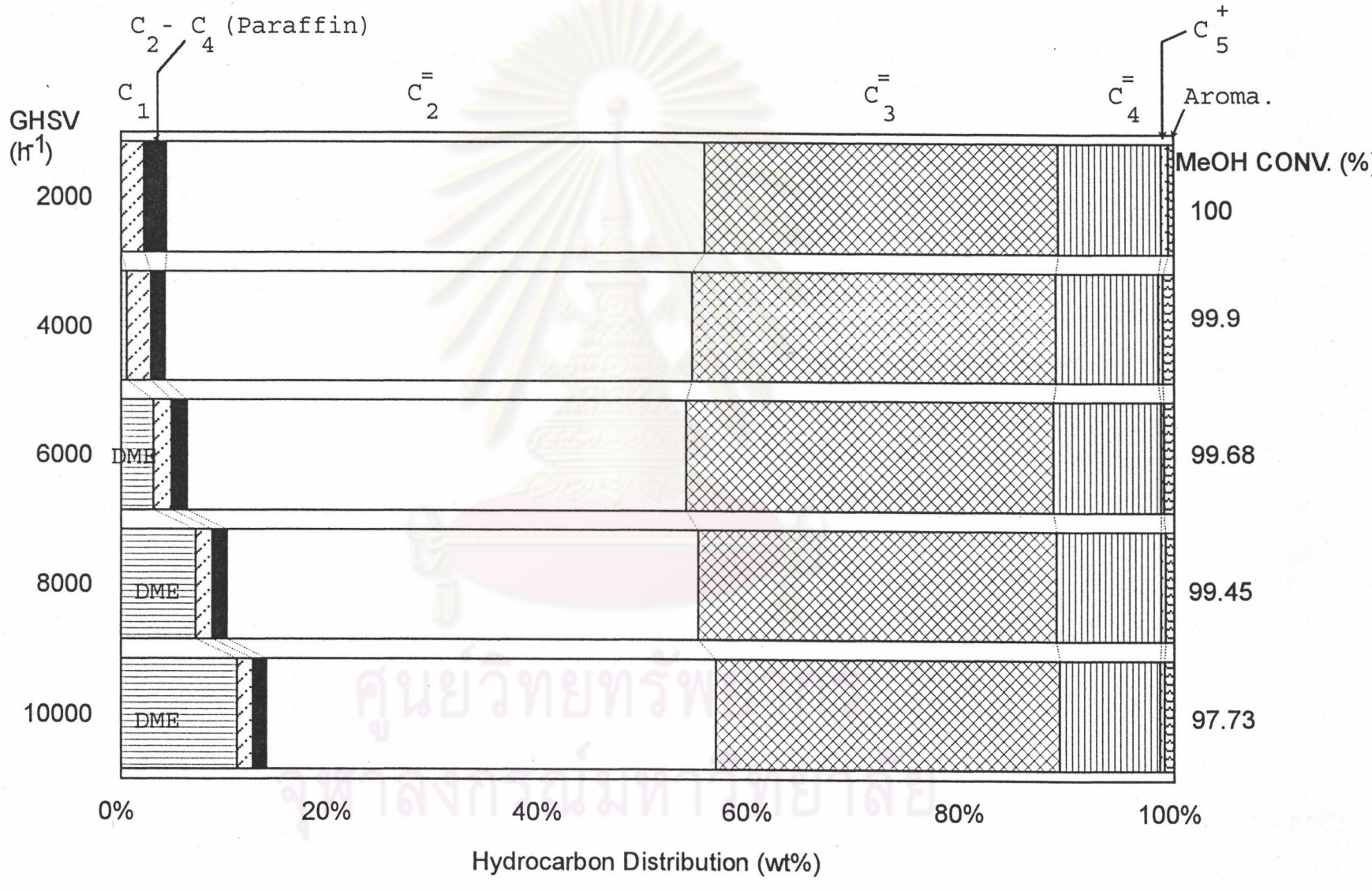

Figure 5.11 Effect of GHSV on the hydrocarbon distribution of methanol conversion on SAPO-34/HF

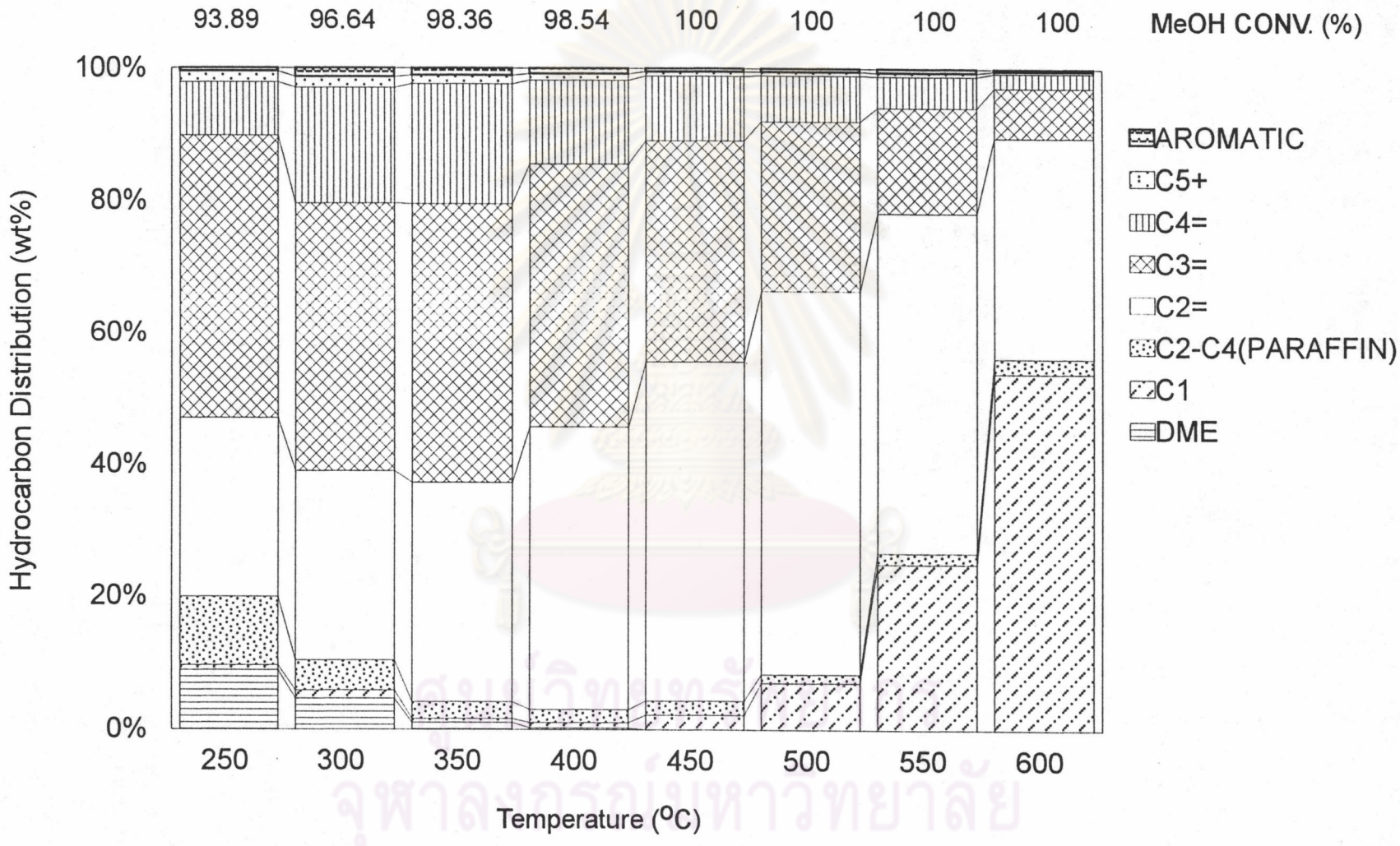

Figure 5.12 Temperature dependence of hydrocarbon distribution of methanol conversion on SAPO-34/HF catalyst.

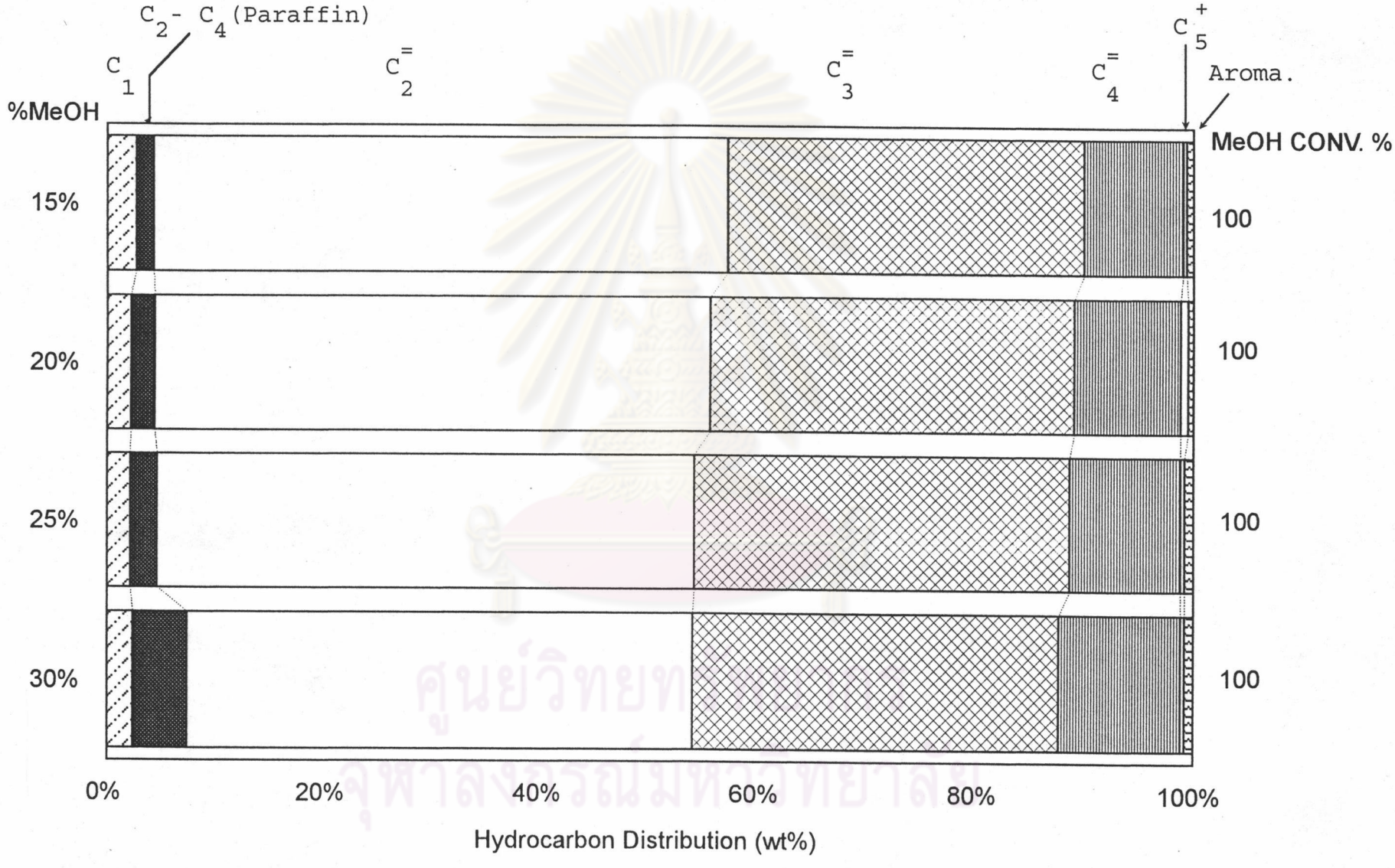

Figure 5.13 Effect of methanol compositions on hydrocarbon distribution of methanol conversion on SAPO-34/HF

Effect of the Presence of Water in Methanol Feed on Ethylene Selectivity

The presence of water in methanol feed was found to markedly enhance the ethylene selectivity as shown in Figure 5.14. The amounts of ethylene increased with the increasing amounts of water and ethylene selectivity as high as 73% was achieved by using feed of H_2O/MeOH ratio of 2. The production of propylene and butenes was suppressed while the selectivity for light olefins ($C_2^=$,$C_3^=$,$C_4^=$) remained almost constant.

It is now generally accepted that the methanol conversion reaction proceeds by the formation of ethylene as the initial olefin product[29]:

$$2CH_3OH \longrightarrow CH_3OCH_3 + H_2O$$

$$2CH_3OCH_3 \longrightarrow CH_2{=}CH_2 + 2CH_3OH$$

Various mechanisms have been proposed for the initial formation of ethylene from methanol and carbonium ion [87], carbenoid species [95], or oxonium ion/oxonium ylide [96] was suspected as the intermediate. However, once ethylene is formed, the reactions proceed by a completely different mechanism. Ethylene is methylated with methyl cation from methanol or dimethyl ether yielding propylene and stepwise methylation of olefins takes place :

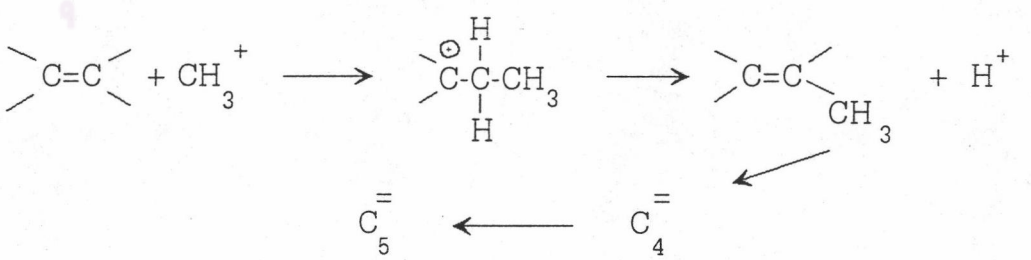

Since the formation of methyl cation is in the equilibrium :

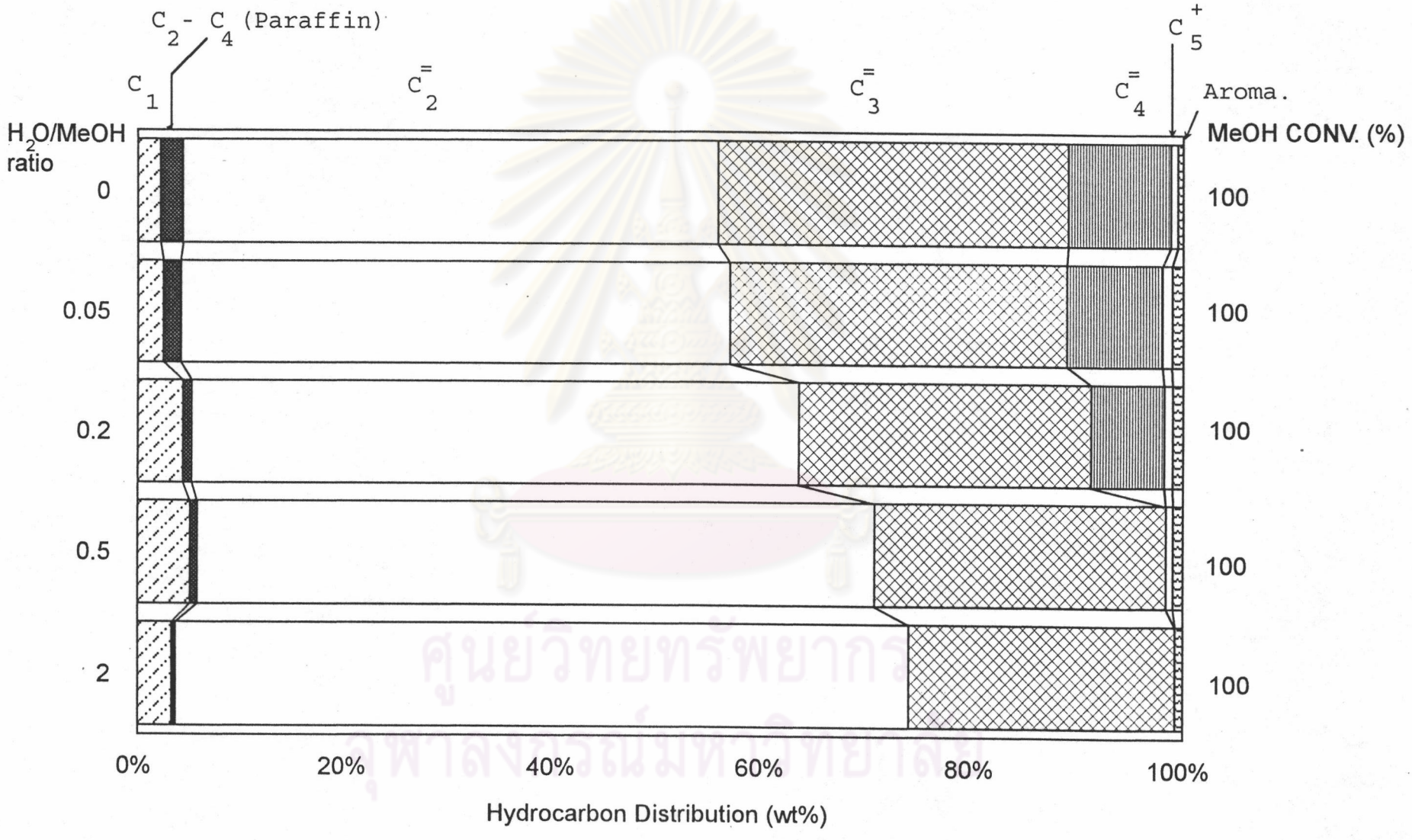

Figure 5.14 Effect of the presence of water in MeOH feed on ethylene selectivity.

$$H^{+} + CH_3OH \rightleftharpoons CH_3^{+} + H_2O$$

adding of water will shift the equilibrium to the left and decrease the steady-state concentration of methyl cation. As a result, the methylation of ethylene to propylene was suppressed which should be responsible for the favorable effect of water on ethylene selectivity.

Effect of Time on Stream on Selectivity for Light Olefins

The stability of SAPO-34 catalyst was tested by prolonged operation as shown in Figure. 5.15. The light olefins selectivity from methanol conversion without any water in the feed decreased rapidly during the 5 h on stream and gradually declined after the period. By contrast with the methanol feed consisting H_2O/MeOH ratio of 2, the decrease of light olefins selectivity during the first period was substantially alleviated. This should be ascribed to the favorable effect of water by acting as an oxidizing agent to burn off the coke formed on the catalyst.

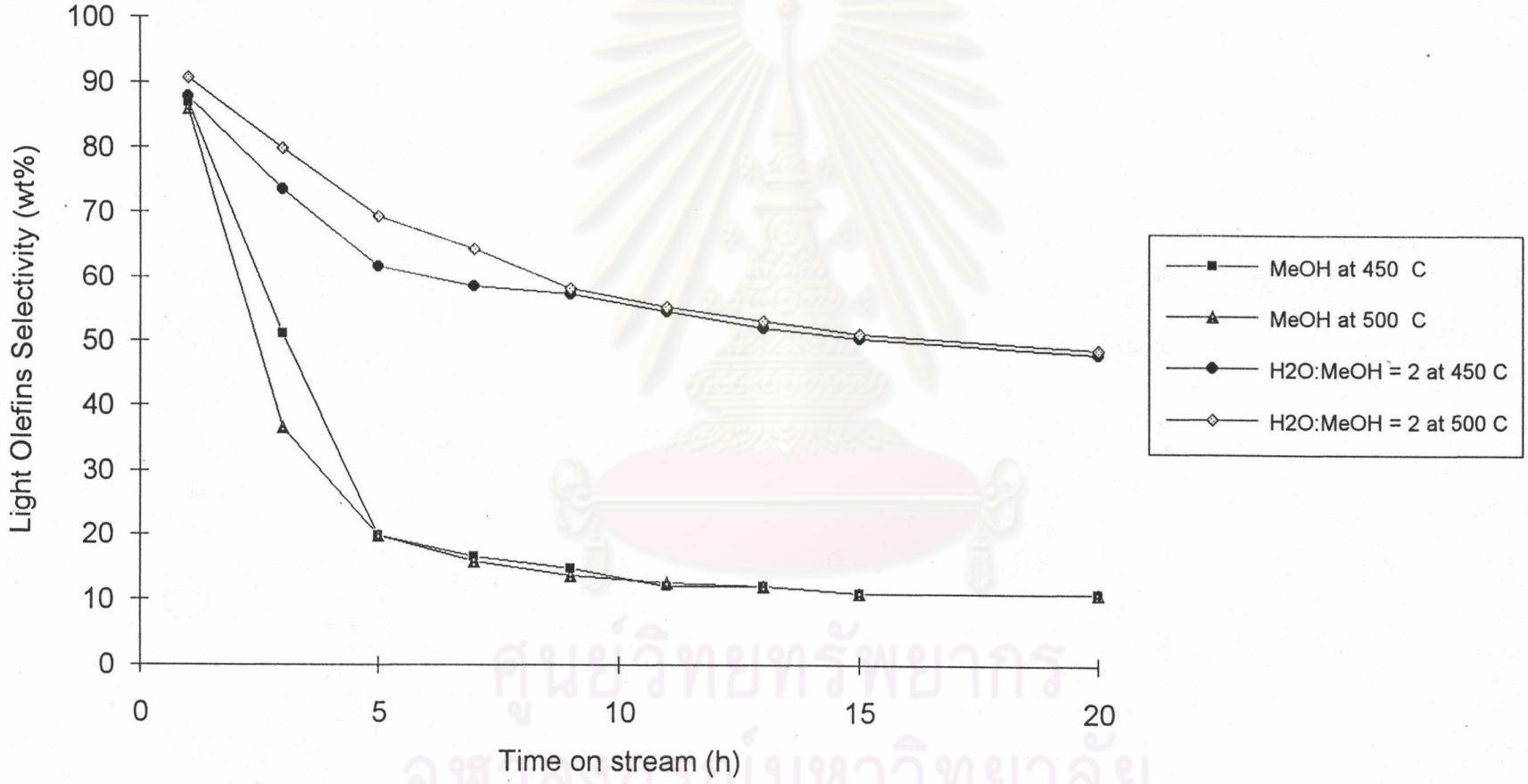

Figure 5.15 Prolonged operation of methanol conversion on SAPO-34 catalyst.